Available online at www.sciencedirect.com
ScienceDirect
Geoderma 145 (2008) 449–461
GEODERMA
www.elsevier.com/locate/geoderma

Modelling coupled water flow, solute transport and geochemical reactions affecting heavy metal migration in a podzol soil

D. Jacques [a,*], J. Šimůnek [b], D. Mallants [a], M.Th. van Genuchten [c]

[a] *Performance Assessment Unit, SCK•CEN, Boeretang 200, B-2400 Mol, Belgium*
[b] *Department of Environmental Sciences, A135 Bourns Hall, University of California Riverside, 900 University Avenue, Riverside, CA 92521, USA*
[c] *U.S. Salinity Laboratory, USDA, ARS, 450 W. Big Spring Rd, Riverside, CA, 92507, USA*

Received 5 April 2007; received in revised form 5 September 2007; accepted 29 January 2008
Available online 10 March 2008

Abstract

Many or most subsurface pollution problems at the field scale involve such simultaneous processes as water flow, multicomponent solute transport, heat transport and biogeochemical processes and reactions. Process-based models that integrate these various processes can be valuable tools for investigating the mobility of a wide range of inorganic and organic contaminants subject to different hydrologic and geochemical conditions. The HP1 reactive transport simulator, obtained by weak coupling of HYDRUS-1D and PHREEQC-2, was developed and designed to address multicomponent geochemical transport processes in the vadose zone. In this paper we discuss a hypothetical HP1 application involving the transport of major cations and heavy metals in a soil during transient flow over a period of 30 years. Results show that variations in water content and water fluxes can significantly influence the speciation, and thus the mobility and availability, of elements. Decreasing water contents near the soil surface lowered pH of the soil solution and produced new cation exchange equilibrium conditions. The upward transport of Cl during summer due to increased evapotranspiration, and subsequent accumulation of Cl near the soil surface, caused an increase in the total aqueous Cd concentration because of the formation of Cd–Cl complexes. Coupled reactive transport codes for the unsaturated zone, such as HP1, are promising tools to unravel the complex interaction between soil physical and biogeochemical processes for all kinds of problems, including the impact of natural processes and antropogenic activities on soil evolution.

Keywords: Reactive transport modelling; Unsaturated zone; Heavy metals

1. Introduction

Process-based reactive transport models can be valuable tools for studying the subsurface fate and transport of organic or inorganic contaminants, including radionuclides, nutrients and pesticides, that may be subject to a large number of often simultaneous interactive physical, chemical, mineralogical, geological, and biological processes (e.g., Mayer et al., 2002; Metz et al., 2002; Davis et al., 2004; Lichtner et al., 2004; Appelo and Postma, 2005; NRC, 2006). Another application involving long-term reactive transport is the genesis of a soil profile from parent material which, besides weathering, includes aqueous complexation and the transport and sorption of chemical species and various clay or organic matter particles. These processes influence mineral precipitation and dissolution, which are the main processes of pedogenesis in the long term (Jenny, 1941; Arkley, 1963; Hoosbeek and Bryant, 1992; Presley et al., 2004; Rasmussen et al., 2005). The concentration of different elements will determine whether parent materials dissolve and secondary minerals form, depending on their saturation status. Some elements also play a role in the solubility or precipitation of organic ligands, or the flocculation of clay particles. Changes in the chemical composition or pH of the soil solution may impact the sorption of elements on organic matter or iron oxides and also affect the saturation index of minerals. Simulation of these and related processes requires a coupled reactive transport code that integrates the physical processes of water flow and advective–

* Corresponding author.
E-mail address: djacques@sckcen.be (D. Jacques).

0016-7061/$ - see front matter © 2008 Elsevier B.V. All rights reserved.
doi:10.1016/j.geoderma.2008.01.009

dispersive solute transport with a range of biogeochemical processes.

An excellent example of the interplay between geochemical conditions and the mobility of elements was given by Jansen et al. (2002) involving the binding of Al and Fe to (mobile) organic matter. Jansen et al. (2002) investigated factors controlling soluble complexation between Fe/Al and dissolved organic matter. Small pH changes (between 3.5 and 4.5) were found to greatly affect soluble complexation of aluminium, ferrous and ferric iron with dissolved organic matter. At a low metal–organic matter ratio, complexation increased with increasing pH due to proton dissociation of the functional groups on the organic matter. However, soluble complexation decreased with increasing pH at a high metal–organic matter ratio due to the formation of insoluble metal–organic matter complexes. Redox conditions are also important for Fe(II) and Fe(III) reactions. As Fe(III)-dissolved organic matter complexes are more stable but less soluble than Fe(II) complexes, Jansen et al. (2002) were able to show that the Fe(III)-dissolved organic matter complexes prevail because of their higher stability at relatively low metal–organic matter ratios, whereas Fe(II)-dissolved organic matter complexes dominate at higher ratios due to the formation of insoluble Fe(III) complexes.

Since element speciation affected by the above and similar interactions significantly influences the mobility and bioavailability of the elements, geochemical speciation calculations should be integrated into the classical vadose zone flow and transport models. At the same time, soils are inherently open systems with changing air and water contents, fluctuating ground water tables and space-time variations in carbon dioxide concentrations. As will be illustrated in this paper, such transient flow conditions also induce changes in pH and speciation (see also Jacques et al., 2006b). To account for these effects, it is necessary to couple all relevant physical and biogeochemical processes that may occur in soil systems. Physical processes involve (i) transient water flow in variably-saturated porous media, (ii) transport of multiple components, and (iii) heat transport. The conceptual models for each of these processes are typically written in terms of partial differential equations and then solved numerically subject to certain initial and boundary conditions. The equations generally also involve a set of constitutive relationships for selected variables or soil properties (e.g., the unsaturated soil hydraulic properties). The definition of a network of (bio)geochemical reactions similarly allows to incorporate the current stage of knowledge on relevant soil (bio)geochemical processes for a specific problem. Multiple kinetic and equilibrium reaction pathways are often a critical feature of such a reaction network (Steefel, 2000). One type of reactions in this approach proceeds then relatively fast as compared to transport, may be path-independent, and usually relates mostly to aqueous complexation reactions and adsorption reactions. A second type of reactions proceeding more slowly as compared to transport processes and to equilibrium reactions may involve oxidation/reduction, biologically mediated reactions, and mineral dissolution/precipitation processes. Since these reactions are path-dependent, both sequential and parallel reactions may be important (e.g., for TNT-degradation pathways; Šimůnek et al., 2006b).

A quantitative approach based on integrating and coupling multiple processes is also useful for pedogenesis modelling, especially for mechanistic modelling at the mesoscopic scale (i.e., the profile, pedon or field-scale) within the hierarchy of soil process modelling as defined by Hoosbeek and Bryant (1992). Soil hydrology is clearly one of the major driving forces of pedogenesis through its control on physical, biological and geochemical processes (Lin, 2003). The term hydropedology (Lin, 2003; Lin et al., 2006) is now frequently used to explicitly stress the interactive nature of pedologic and hydrologic processes in the vadose zone. Geochemical processes in turn may affect also the physical and hydraulic properties of soils, including porosity and permeability (e.g., Lapen and Wang, 1999; Mecke et al., 2000). For saturated conditions, some macroscopic (e.g., the Carmen–Kozeny, Brinkman or Fair–Hartch models as discussed by Le Gallo et al., 1998) or grain-scale (e.g., Panda and Lake, 1995) models are available for this purpose. Similar models have also become available for the unsaturated hydraulic properties (Freedman et al., 2004). Alternatively, pedotransfer functions relating basic soil physical properties to the unsaturated soil hydraulic functions could be used to update the hydraulic properties (e.g., Finke, 2006).

The objective of this paper is to discuss the importance of variations in soil water contents and water fluxes on element mobility as illustrated by a hypothetical numerical example implemented in a coupled reactive transport code integrating the different physical and biogeochemical processes.

2. Coupling geochemical reactions with water flow and solute transport

2.1. Mathematical description of transport and geochemical processes

This section defines some governing equations for the physical (transport) and the biogeochemical processes used in a mechanistic-based reactive coupled transport code. The overview is limited to the processes used in the numerical example discussed further. A more complete overview of involved processes and their mathematical treatment is given e.g. in Lichtner (1996) and in the documentation of different coupled codes (e.g., 3DHYDROGEOCHEM, Yeh and Cheng, 1999; MIN3P, Mayer et al., 2002; HP1, Jacques and Šimůnek, in preparation).

The geochemical processes used in the example are aqueous complexation and ion exchange. The aqueous complexation reactions are written in terms of components or master species and their stoichiometric coefficients (Morel and Hering, 1993). The general reaction equation for an aqueous species is:

$$\sum_{j=1}^{N_m} v_{ji} A_j^m = A_i \tag{1}$$

where N_m is the number of aqueous master species, $i=1,\ldots, N_{sa}$, N_{sa} is the number of aqueous secondary species, A_j^m and A_i are the chemical formula for the master and secondary species, respectively, and v_{ji} are the stoichiometric coefficients in the reaction. At equilibrium (i.e., when the free energy of the

system is at a minimum), the mass law equations together with the component conservation equations allow calculation of the speciation. The mass law equations are:

$$K_i^l = a_i^l \prod_{j=1}^{N_m} \left(a_j^m\right)^{-v_{ji}^l} \quad (2)$$

where K_i^l is the thermodynamic equilibrium constant [−], a is the activity [−] defined as $a_i = \gamma c_i / c_i^0$ where c is the molal concentration [mol kg^{-1} water], c_i^0 is the standard state (i.e. 1 mol kg^{-1} water, Appelo and Postma, 2005), γ is the activity coefficient [−], and the superscript m and l refers to master and secondary aqueous species. The activity coefficient is calculated with the extended Debye–Hückel equation (Langmuir, 1997; Parkhurst and Appelo, 1999).

From the different models to describe sorption on the solid soil phase (e.g., linear, Freundlich or Langmuir equilibrium sorption isotherms, cation (or anion) exchange and surface complexation models), the ion exchange model is used, written in the Gaines and Thomas' (1953) convention:

$$\sum_{j=1}^{N_m} v_{ji_e}^e A_j^m + v_{j_e i_e}^e X_{j_e}^m = A_{i_e}^e \quad (3)$$

where $j_e = 1,\ldots, N_X$ (N_X is the number of master exchangers), $i_e = 1,\ldots, N_{se}$ (N_{se} is the number of the secondary exchange species), and the superscript e refers to exchange reactions. Let the activity of an exchange species be defined as

$$a_{i_e} = \gamma_{i_e}^e \beta_{i_e, j_e} \quad (4)$$

where a is the activity [−], $\gamma_{i_e}^e$ is the activity coefficient of the i_eth exchange species [−], and β_{i_e,j_e} is the equivalent fraction of the i_eth exchange species on the j_eth exchanger [−]. The mass-action equations for equilibrium conditions can now be written as

$$K_{i_e}^e = \gamma_{i_e}^e \beta_{i_e,j_e} \prod_{j=1}^{N_m} \left(\gamma_j^m c_j^m\right)^{-v_{ji_e}^e} \left(\gamma_{j_e}^e \beta_{j_e,j_e}\right)^{-v_{j_e i_e}^e}. \quad (5)$$

The physical processes used in the example are water flow and solute transport. The water flow equation is based on conservation of mass within a given soil volume and on the summation of fluxes in and out of this volume. The fluxes are described with the Darcy–Buckingham law relating the flux in the unsaturated soil to the pressure head gradient in the soil and a moisture dependent proportionality factor. The resulting Richards equation for water flow in soils is:

$$\frac{\partial \theta(h)}{\partial t} = \frac{\partial}{\partial x}\left[K(h)\left(\frac{\partial h}{\partial x} + \cos\alpha\right)\right] - S(h) \quad (6)$$

where h is the soil water pressure head [L], θ is the volumetric water content [L^3L^{-3}], t is time [T], x is the spatial coordinate [L] (positive upward), S is the sink term [$L^3L^{-3}T^{-1}$], α is the angle between the flow direction and the vertical axis, and K is the unsaturated hydraulic conductivity [LT^{-1}]. To describe the relations between θ–h and K–h, the van Genuchten equations (van Genuchten, 1980) are used:

$$\theta(h) = \theta_r + \frac{\theta_s - \theta_r}{(1 + |\alpha h|^n)^m} \quad (7)$$

and

$$K(h) = K_s S_e^l \left[1 - \left(1 - S_e^{1/m}\right)^m\right]^2 \quad (8)$$

where θ_r is the residual water content [L^3L^{-3}], θ_s is the saturated water content [L^3L^{-3}], α [L^{-1}], n [−] and m ($=1-1/n$) [−] are shape parameters, l is a pore connectivity parameter [−], K_s is the saturated hydraulic conductivity [LT^{-1}], and $S_e = (\theta - \theta_r)/(\theta_s - \theta_r)$ is the effective saturation.

For equilibrium aqueous complexation reactions, it is convenient to transport only total concentrations which are defined as:

$$C_j = c_j + \sum_{i=1}^{N_{sa}} v_{ji} c_i. \quad (9)$$

Assuming that all diffusion coefficients are equal (i.e., species-independent diffusion), the advection–dispersion equation that combines the mass conservation equation with Fick's diffusion law can be written for each component as follows (see also Lichtner, 1996; Mayer, 1999):

$$\frac{\partial \theta C}{\partial t} = \frac{\partial}{\partial x}\left(\theta D^w \frac{\partial C_j}{\partial x}\right) - \frac{\partial q C_j}{\partial x} - S C_{r,j} + R_{o,j} \quad (10)$$

where S the sink term in the water flow equation [$L^3L^{-3}T^{-1}$], $C_{r,j}$ is the total concentration of the sink term [ML^{-3}], D^w is the dispersion coefficient in the liquid phase [L^2T^{-1}], and $R_{o,j}$ is the source/sink term that represents various heterogeneous equilibrium and kinetic reactions (e.g., cation exchange, surface complexation, mineral dissolution) and homogeneous kinetic reactions (e.g., degradation reactions in the aqueous phase) [$ML^{-3}T^{-1}$].

The dispersion coefficient D^w in Eq. (10) is given by

$$\theta D_i^w = D_L |q| + \theta D_{i,w} \tau_w \quad (11)$$

where $D_{i,w}$ is the molecular diffusion of the ith aqueous species in free water [L^2T^{-1}], D_L is the longitudinal dispersivity [L], and τ_w is a tortuosity factor in the liquid phase [−] that is related to the water content by the model of Millington and Quirk (1961).

2.2. HP1 simulator

All calculations discussed in this paper were carried out with version 2.0 of HP1 (Jacques et al., 2006b). HP1 integrates a broad range of physical and biogeochemical processes as described in the original manuals of HYDRUS-1D (Šimůnek et al., 2005), PHREEQC-2 (Parkhurst and Appelo, 1999), and HP1 (Jacques and Šimůnek, in preparation). HYDRUS-1D was originally designed mostly for simulating water flow, solute transport and heat transport in soils from the soil column scale, to the lysimeter scale, and the field scale. Important to note is that the model accounts for soil heterogeneity at the macroscopic scale by defining distinct soil horizons, at the small-scale by using scaling factors (Vogel et al., 1991), and at the microscopic scale by using the dual porosity or mobile/immobile flow models (Šimůnek

Table 1
Soil hydraulic properties of the six soil horizons of a sandy dry Spodosol (Seuntjens, 2000)

Horizon	Layer thickness (cm)	θ_r	θ_s	α (cm^{-1})	n	K_s (cm day^{-1})	l
A	13	0.065	0.476	0.016	2.411	93	0.5
E	10	0.035	0.416	0.015	2.446	311	0.5
Bh1	8	0.042	0.472	0.016	2.197	39	0.5
Bh2	8	0.044	0.455	0.028	2.010	860	0.5
Bh/C	16	0.039	0.464	0.023	2.534	1198	0.5
C	45	0.029	0.408	0.039	2.071	1212	0.5

et al., 2003). PHREEQC-2 stems mostly from the field of low-temperature aquatic chemistry and geochemistry. The generic nature of PHREEQC-2 and its flexibility in defining the kinetic reactions with respect to the reaction network, influencing factors and mathematical formulation provide many opportunities to define and include pedogenetic processes. The combination of the advection–dispersion equation with the generic reaction term $R_{o,j}$ in Eq. (10) allows also the description of the movement of colloids (e.g. DeNovio et al., 2004; Šimůnek et al., 2006a). Version 2.0 couples version 3.0 of HYDRUS-1D to solve the water flow, heat transport and solute transport equations, and version 2.13 of PHREEQC to calculate $R_{o,j}$ in Eq. (10), aqueous complexation and the composition of the ion exchange complex.

HP1 implements a weak coupling method in which the governing equations for water flow, heat transport and solute transport are solved sequentially. The multicomponent reactive transport equations are solved using a non-iterative sequential approach, meaning that the physical part is solved first without any chemical interactions, while the chemical reactions that are uncoupled in space and coupled over the components are solved subsequently. A flow chart of the operator-splitting approach used in HP1 was given in Jacques et al. (2006a). Although operator-splitting errors may occur with our approach (e.g., Carrayrou et al., 2004), Jacques et al. (2006a) showed that very accurate results can be obtained by carefully selecting the spatial and temporal discretizations for the numerical solution. We refer to Jacques et al. (2006a) for specific discretization guidelines. HP1 is freely available at www.pc-progress.cz.

3. Transient flow and transport of major cations and heavy metals in a soil profile

As an illustrative example, HP1 is used in this section to simulate the leaching of Cd and Zn in a dry Spodosol in a sandy region of Northern Belgium using in-situ measured Cd and Zn (and additional elements) concentration profiles. Soils in the region were contaminated by atmospheric deposition of Cd and Zn from non-ferrous industry (Seuntjens, 2000). Water flow and the transport of major cations (Na, K, Mg, and Ca), heavy metals (Cd and Zn), anions (Cl, Br) and Al were simulated for a 1-m deep multi-layered soil profile subject to atmospheric boundary conditions for a period of 30 years. Our main focus here is on how processes affecting water contents and water fluxes also influence the geochemical conditions in the soil. Specifically, the effect of cycles of evaporation and infiltration on pH and Cd speciation will be discussed in detail.

3.1. Problem definition and model input

The experimental site "Kattenbos" is located in the community of Lommel (Belgium) at a distance of about 2 km east from a metallurgical plant. Various soil parameters and the initial conditions were taken from Seuntjens (2000). The dry Spodosol consists of six horizons, with a typical leached E-horizon between 13–23 cm below the soil surface, and enriched (organic matter and Fe-oxides) Bh-horizons between 23–55 cm below the surface. Table 1 gives depths, parameters of the water retention characteristics, $\theta(h)$, and the saturated hydraulic conductivity, K_s, (both measured in the laboratory on core samples of 100 cm^3) for each soil layer.

Interactions between major cations and heavy metals with the soil solid phase were simulated by means of cation exchange processes assuming local equilibrium on a single type of exchange sites. Voegelin (2001) has shown that this approach adequately describes various features of Cd transport experiments. Although sorption on specific sites with a high affinity for Cd may also occur in soils (Selim et al., 1992), this type of binding is unlikely in acid sandy soils (Smolders et al., 1999; Voegelin et al., 2001). Exchange parameters were calibrated using concentrations measured in drainage water from a steady-state flow experiment on large, undisturbed soil lysimeters (1-m-long and 0.8-m-diameter, Seuntjens et al., 2001). The initial composition of the cation exchange site was measured for each soil horizon (Table 2). Resulting exchange parameters are given in Table 3. While the same log(K) parameters were used for all soil horizons, the size of the cation exchange complex was assumed to vary between horizons. We note that Al in the soil profile was assumed to be in equilibrium with Gibbsite ($Al(OH)_3$). This resulted in a good description of the measured pH and Al in the drainage water (results not shown).

The initial aqueous concentrations were obtained by equilibrating the soil solution with the cation exchange composition.

Table 2
Initial composition of the cation exchange sites (in mol/1000 cm^3 soil) (Seuntjens, 2000)

Horizon	HX	NaX	KX	CaX_2	MgX_2	CdX_2	ZnX_2
A	$1.32\ 10^{-2}$	$2.73\ 10^{-4}$	$2.99\ 10^{-4}$	$2.77\ 10^{-4}$	$1.44\ 10^{-4}$	$1.52\ 10^{-5}$	$2.00\ 10^{-4}$
E	$8.76\ 10^{-3}$	$2.90\ 10^{-4}$	$2.03\ 10^{-4}$	$1.57\ 10^{-4}$	$7.26\ 10^{-4}$	$1.70\ 10^{-5}$	$8.20\ 10^{-5}$
Bh1	$1.78\ 10^{-2}$	$5.36\ 10^{-4}$	$4.89\ 10^{-4}$	$5.00\ 10^{-4}$	$2.38\ 10^{-4}$	$4.51\ 10^{-5}$	$3.64\ 10^{-4}$
Bh2	$1.29\ 10^{-2}$	$2.41\ 10^{-4}$	$2.81\ 10^{-4}$	$1.86\ 10^{-4}$	$1.24\ 10^{-4}$	$1.84\ 10^{-5}$	$2.45\ 10^{-4}$
Bh/C	$3.61\ 10^{-3}$	$4.42\ 10^{-4}$	$1.20\ 10^{-4}$	$1.24\ 10^{-4}$	$5.80\ 10^{-5}$	$1.38\ 10^{-5}$	$4.64\ 10^{-5}$
C	$4.80\ 10^{-3}$	$9.05\ 10^{-5}$	$2.01\ 10^{-4}$	$3.85\ 10^{-5}$	$6.34\ 10^{-5}$	$1.25\ 10^{-5}$	$1.84\ 10^{-5}$

Table 3
Log K parameters for the cation exchange reactions

Formula	Log K
$X^- + H^+ = HX$	4.2
$X^- + Na^+ = NaX$	1.8
$X^- + K^+ = KX$	2.85
$X^- + Ca^{2+} = CaX_2$	2.8
$X^- + Mg^{2+} = MgX_2$	3.1
$X^- + Cd^{2+} = CdX_2$	4.0
$X^- + Zn^{2+} = ZnX_2$	2.85

Element concentrations in the rain water were obtained from Stolk (2001) for station 231 located in Gilze-Rijen (the Netherlands) close to the site investigated here. The composition was based on the average of 13 measurements during 1999 (Table 4). The cation exchange sites were initially not in equilibrium with the composition of the rain water. Consequently, long-term changes in the composition of the cation exchange sites were simulated for a period of 30 year, not only for Cd and Zn (due to infiltration of heavy metal free water), but also for the other major cations.

Atmospheric boundary conditions were taken for the soil surface (see further), whereas a free drainage (a zero pressure head gradient) was taken as the bottom boundary condition.

3.1.1. Precipitation and potential evaporation

Climatological data were taken from two nearby weather stations (from Brogel for years 1969 through 1985, and from Mol/Geel for years 1986 through 1998). The potential evaporation, E_p [L T^{-1}], was calculated using the Penman equation (Penmann, 1948).

The total precipitation during the 30-year simulation period was 24,933 mm with a mean of 831 mm/year and a standard deviation of 152 mm/year. The maximum and minimum yearly precipitation was, respectively, 494 mm (1976) and 1169 mm (1998). The mean and standard deviation of the potential evaporation was 477 mm/year and 91 mm/year, respectively, with 329 mm (1979) and 616 mm (1990) as minimum and maximum values, respectively. This results in a mean yearly potential precipitation surplus P_p^*, defined as the difference between the precipitation P and the potential evaporation E_p, of 353 mm/year, varying between 32 (1976) and 621 (1988) mm. Fig. 1 shows the cumulative potential precipitation surplus flux between 1972 and 1981. During the summer months of 1975 and 1976, P_p^* was close to zero. An overview of the monthly positive and negative P_p^* is given in Fig. 2. On a monthly basis, at least 25% of months between April and August had a negative potential precipitation surplus. The actual evaporation rate, E_a [LT^{-1}], was lower than the potential rate (10,473 mm versus 14,335 mm), resulting in a higher actual precipitation surplus (Fig. 1). The large difference is due to the absence of plant roots in this example. The sandy soil with its low hydraulic conductivity when dry was unable to provide enough water to satisfy the atmospheric demand, leading to lower E_a fluxes.

Table 4
Chemical composition of the rain water (from Stolk, 2001) (*: charge balance)

Concentration (μmol/l)	pH	Cl	Br*	Na	K	Ca	Mg	Cd	Zn
Rain water	5.25	69	32	64	4	6	8	0	0

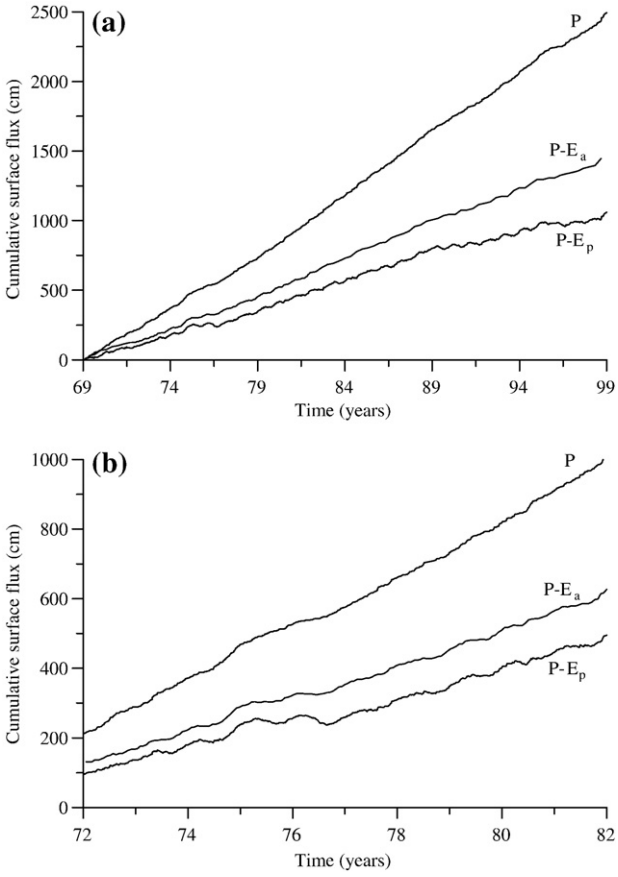

Fig. 1. Cumulative potential and actual precipitation surplus for the 30-year period (a) and a detail for the period 1972–1981 (b).

3.1.2. Spatial and temporal discretization

Spatial and temporal discretizations leading to minimal operator-splitting errors were determined using the guidelines

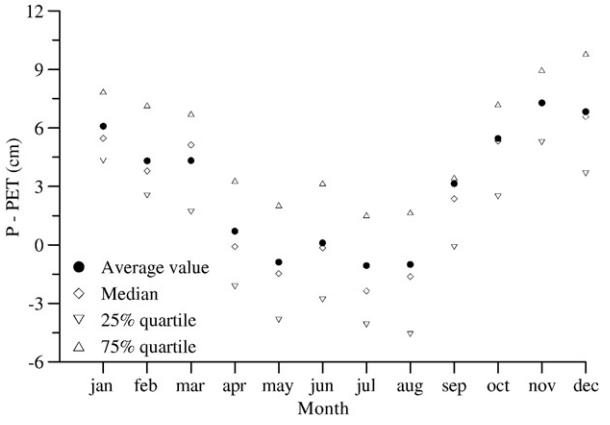

Fig. 2. Statistics of the monthly potential precipitation surplus for the period 1969–1998.

proposed by Jacques et al. (2006a). Simulations were first carried out for a shorter 3-year time period (1975–1977) involving alternating wet and dry periods, with at least one very dry period having a relatively high potential evapotranspiration rate, ET_p, to optimise the maximum time step and the performance index ω_s obtained by multiplying the Peclet and Courant numbers. We found that smaller maximum time steps were most effective for reducing operator-splitting errors during periods with larger evapotranspiration rates, whereas decreasing the performance index was most effective during water infiltration periods. A simulation with Δx=0.5 cm, ω_s=0.125, and a maximum allowed time step of 0.125 day was used as the reference run. Nine other simulations were carried out with a spatial discretization of 1 cm and different maximum allowed time steps (0.5, 0.25 and 0.125 day) and ω_s values (0.4, 0.2 and 0.1). Since it is likely that the reference run may also produce larger errors during relatively dry periods, the accuracy of different simulation runs was assessed by comparing simulation results for periods with high precipitation rates and low evaporation rates (i.e., during winter) to optimize ω_s. Evaluated over all chemical components, the lowest tested ω_s value was selected (with a maximum time step of 0.125 day). To optimize the maximum allowed time step, the maximum difference between the reference run and simulations with different maximum time steps was determined. Our current example required a maximum time step of 0.125 day. For a similar problem over a 10-year simulation period (1972–1982), the relative error in the solute mass balance (using Δx=1 cm, ω_s=0.1, and a maximum time step of 0.125 day) was calculated using Eq. (8.55) of Šimůnek et al. (2005) for consecutive time intervals of 15 days. The errors were consistently less than 1%, which indicates that the HP1 mass balance errors were relatively small for our example (see Jacques and Šimůnek, in preparation).

3.2. Simulation results

Detailed simulation results for the year 1975 are presented in Figs. 3–6. On an annual basis, 1975 had the sixth lowest P_p^*. The year 1975 was chosen because it has relatively distinct periods with mainly positive and negative potential precipitation surpluses, as shown in Fig. 3. This year could be divided into three periods: period I (12/27/1974–04/20/1975) with mostly positive values of P_p^*, period II (04/20/1975–09/20/1975) with mostly negative values of P_p^*, and period III (09/20/1975–01/09/1976)) with mostly positive values of P_p^*. This division was made to relate accumulation and leaching of the different elements to time periods with either positive or negative potential precipitation surpluses.

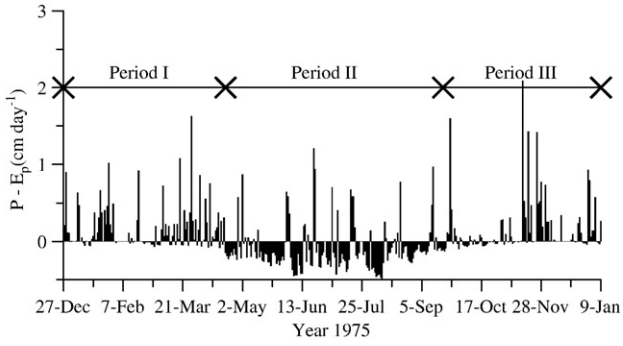

Fig. 3. Potential precipitation surplus of year 1975 (12/27/1974–01/09/1976).

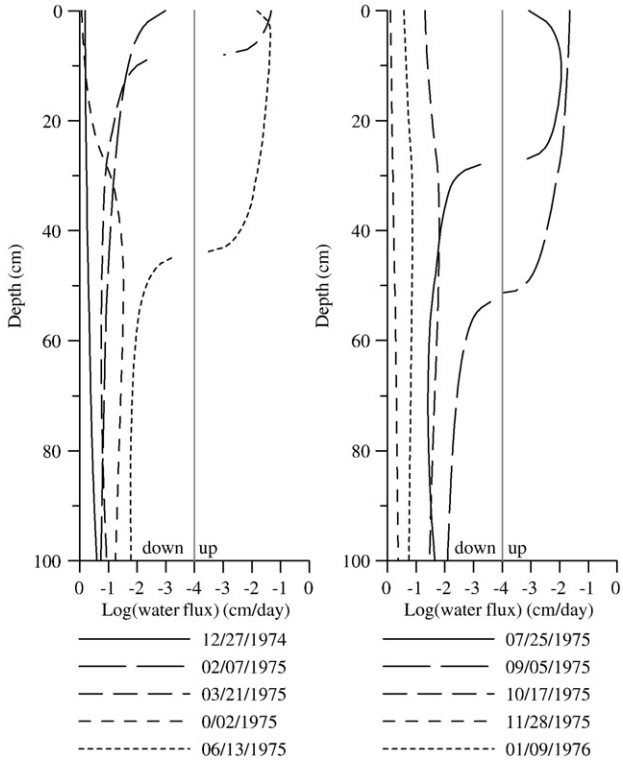

Fig. 4. Water fluxes in the soil during year 1975 (12/27/1974–01/09/1976).

3.2.1. Water fluxes during 1975

Water fluxes in the soil profile during the period 12/7/1974 to 01/09/1976 are shown in Fig. 4. As expected, the highest variability in the water flux occurred in the top soil, ranging from a 0.8 cm day^{-1} downward flux to a 0.047 cm day^{-1} upward flux. During evaporation periods, the zone with upward flow propagated down to a depth of 50 cm in the soil profile.

3.2.2. Cl, Na, Ca, and Cd concentrations at different depths during 1975

To circumvent the effect of changing water contents on the concentrations, we expressed concentrations in terms of mass per soil volume (mol/1000 cm^3 of soil) instead of liquid concentrations (mol/l). Fig. 5 shows the change (compared to the first date of 03/21/1975) in the total mass of Cl, Na, Ca and Cd (T_X in mol/1000 cm^3) in three soil compartments (0–9 cm, 20–29 cm, and 40–49 cm) for a limited time period (03/21–11/28) during 1975. For Na, Ca and Cd, T_X represents the sum of the aqueous and adsorbed amounts. The cumulative inflow of Cl, Na, and Ca from the rain water in the top compartment is also plotted.

The results in Fig. 5 indicate a strong correlation between the accumulation and leaching of Cl in the first compartment with the precipitation surplus. Periods with a negative P_p^* caused an upward Cl flux and an increase in T_{Cl} in the first compartment. The contribution of Cl from rain water when P_p^* is negative was small. During rainstorms (positive P_p^*), the Cl amount first increased, but then decreased since Cl is subsequently leached from the first compartment. Although deeper in the soil (e.g., 20–29 cm), where Cl fluxes are still upwards during periods with negative P_p^* (not shown), T_{Cl} is decreasing. Upward Cl fluxes are found down to a depth of 50 cm for the year 1975.

The total amount of Na, T_{Na}, exhibits a similar behaviour. However, Na is less mobile than Cl due to the exchange processes. The upward Na fluxes and thus the Na accumulation in the first compartment are slightly smaller than those for Cl. More importantly, leaching during positive P_p^* periods was less, resulting in a larger net increase in Na than in Cl during period I in 1975. A slightly different pattern was simulated for Ca, a less mobile element than Na. During period I, T_{Ca} increased in the upper compartment, whereas T_{Na} (and T_{Cl}) were relatively constant. During period II, changes in T_{Ca} when P_p^* was positive were comparable or larger than when P_p^* was negative. The opposite was simulated for Na. While the difference in Na and Ca mobility during period I can be explained by the increased retardation of Ca (and thus its lower leaching rate), the differences cannot be similarly explained during the second period. This phenomenon is related to changing concentrations of different cations due to variations in water contents and fluxes and the competition of cations with different affinities for the exchange complex (further discussed below). Cd behaved similarly as Ca, but without the accumulation in the first compartment for positive P_p^* values since the rain water did not contain any Cd.

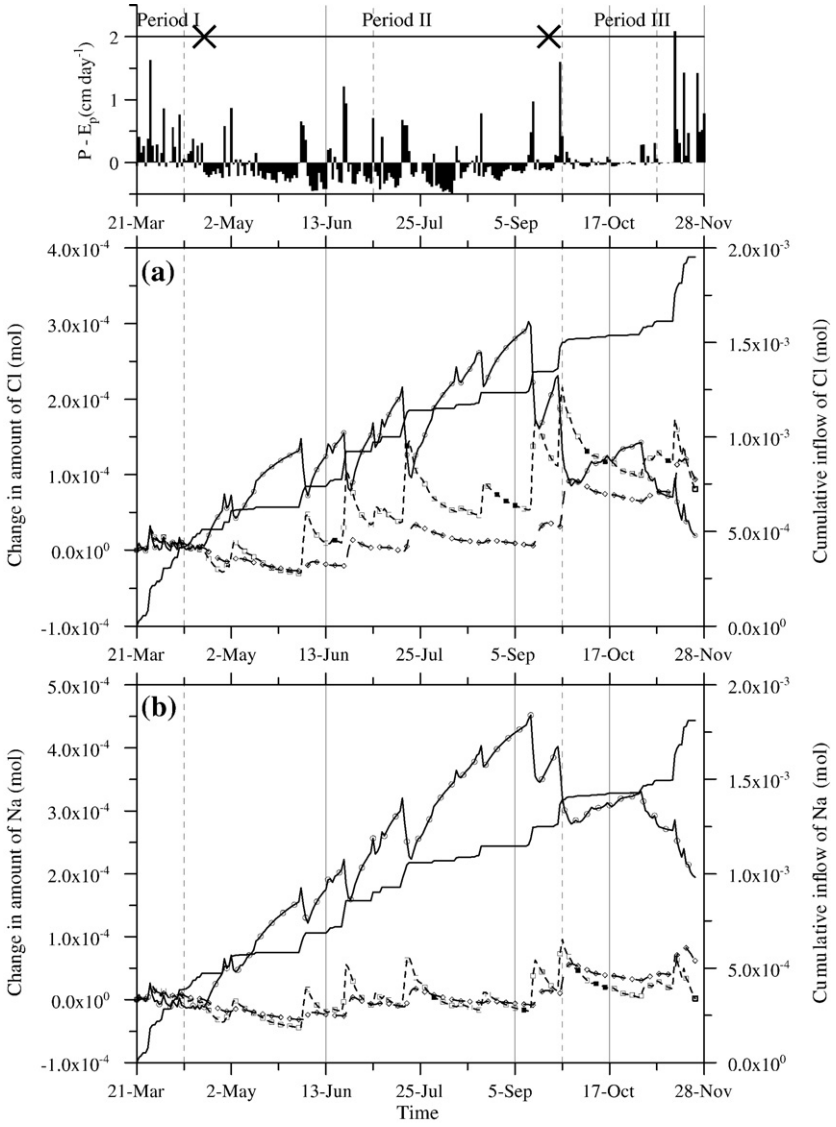

Fig. 5. Changes in amount of (a) Cl, (b) Na, (c) Ca, and (d) Cd (mol/1000 cm^3 soil) in the soil between 0–9 cm (full line, circles), 20–29 cm (short dashes, squares) and 40–49 cm (long dashes, diamonds). For Cl, Na, and Ca the cumulative inflow in the rain water is shown as a full line (on the right axis, note the different scale). The precipitation flux is shown on the top.

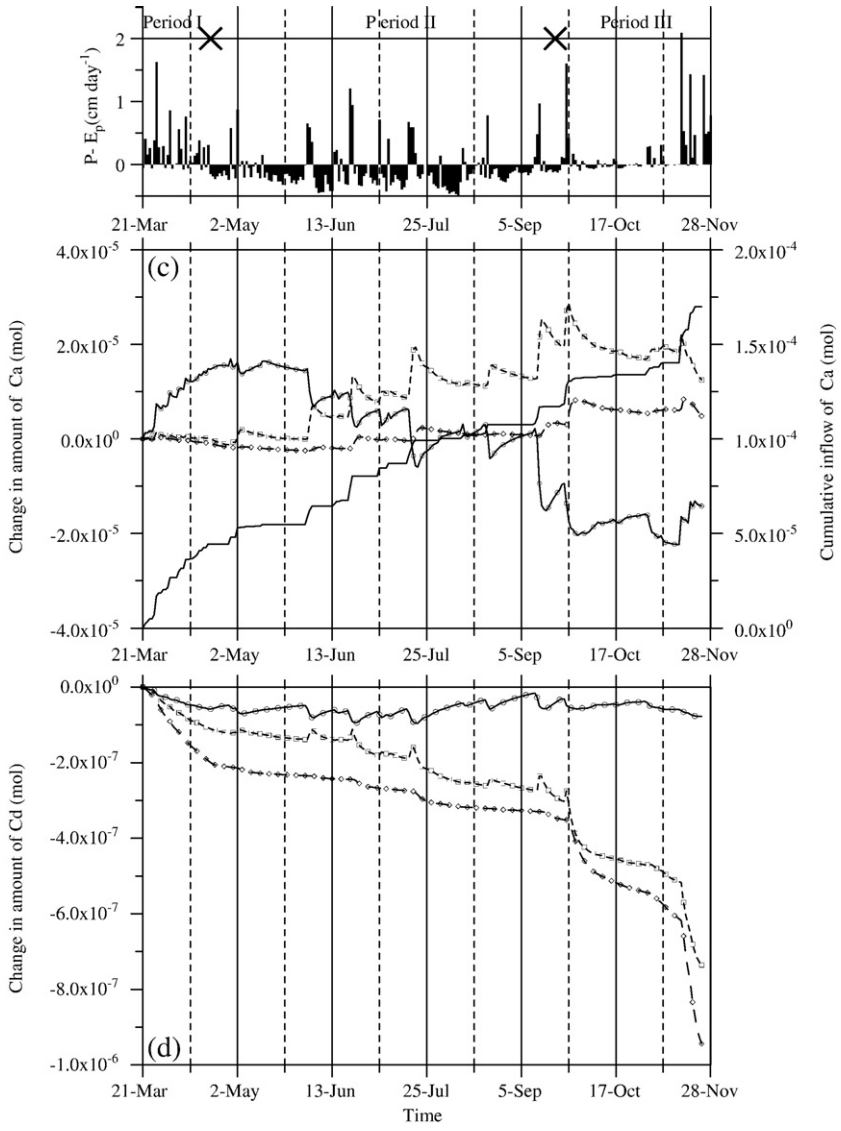

Fig. 5 (*continued*).

3.2.3. Distributions of Na, Ca, and Cd versus depth during 1975

Fig. 6 shows distributions versus depth of total Cl, Na, Ca and Cd in the aqueous phase ($T_{X,aq}$, X=Cl, Na, Ca, Cd). The distributions of Cl illustrate the findings from the mass balance analysis. During the first half of the year (from winter to summer), chloride accumulated in the top soil due to limited downward water flow (e.g., during period II for 1975) and only slowly leached into the bottom half of the soil profile. $T_{Na,aq}$ increased up to 2.5 times in the beginning of period II in 1975, but then remained more or less constant. On the other hand, $T_{Ca,aq}$ in the top soil increased more continuously up to 5 times at the end of period II compared to the beginning of period II. $T_{Na,cec}$ increased during the summer months, whereas $T_{Ca,cec}$ remained relatively constant (results not shown; see Fig. 7 for long-term variation). $T_{Cd,aq}$ showed a strong correlation with the chloride dynamics (in contrast with Ca): on 11/28/1975, $T_{Cd,aq}$ in the subsoil was as high as the highest values in the top soil during the summer, whereas this was not the case for Ca. During the summer months the correlation with Cl was less clear in the top 15 cm: while $T_{Cl,aq}$ increased towards the soil surface, $T_{Cd,aq}$ remained more or less constant. $T_{Cd,cec}$ did not change over one year (results not shown; see Fig. 7). Since $T_{Cd,cec}$ was much larger than $T_{Cd,aq}$ (1.0×10^{-5}–4.0×10^{-5} and 1.0×10^{-9}–1.0×10^{-8} mol Cd, respectively), the total Cd content remained also constant during one year.

3.2.4. Long term changes in total mass (1969–1998)

The variability in the mass of a component in the aqueous phase within a single year was found to be much larger than the long-term variability over 30 years. A slight increase or decrease occurred over the 30 year period, corresponding to an increase or decrease in the adsorbed amounts. The total mass of Na, Ca, and Cd in the different horizons over the period of 30 year is plotted in Fig. 7. For Na, variations in the top horizon (horizon A) within a year were similar to the long-term variations, while for the other horizons the 30-year variability was larger than the variations within one year. However, much of the variation over

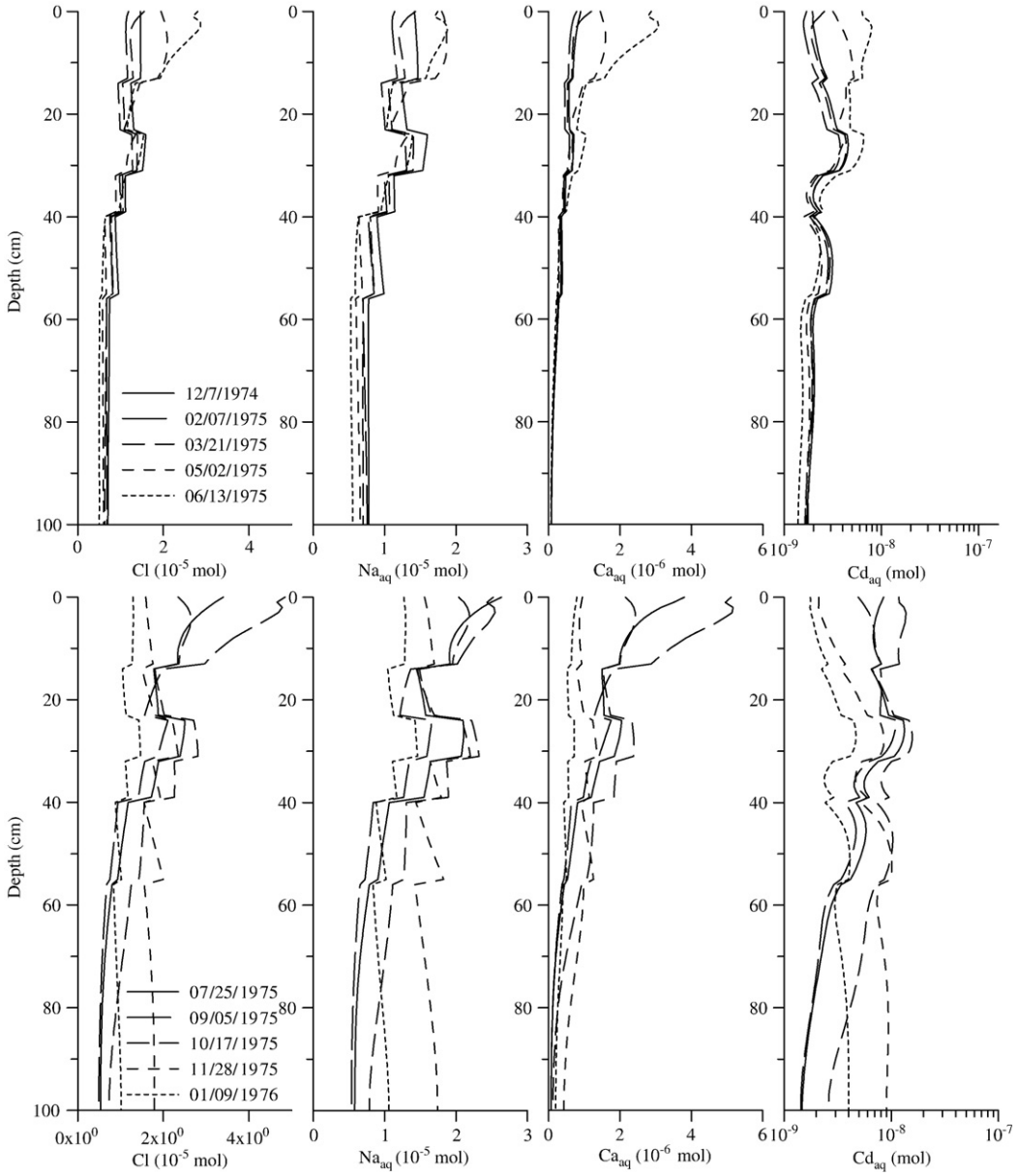

Fig. 6. Distributions versus depth of $T_{Cl,aq}$, $T_{Na,aq}$, $T_{Ca,aq}$ and $T_{Cd,aq}$ (mol/1000 cm^3 soil) at 10 times during year 1975 (12/27/1974–01/09/1976).

the 30 year period was due to disequilibrum between the composition of the rainwater and the initial composition of the cation exchange sites. It took almost 10 years to equilibrate each horizon with the inflowing water. After that, no long-term trend was present anymore, and the within-year variability also increased for the deeper horizons.

Almost no changes were found within one year in the total amounts of Ca and Cd. Long-term changes occurred for Ca during the 30-year simulation period. We found substantial accumulation of Ca (and Mg, results not shown) in the top horizon, accompanied by a decrease in proton-occupied cation exchange sites (results not shown). The change in T_{Cd} in the Ap-horizon was small. Net leaching of Cd occurred in the E and Bh1 horizon, resulting in Cd accumulation in the Bh2 horizon. Cd leached also from the B/C horizon, while accumulating in the upper part of the C-horizon.

3.3. Discussion

Fig. 8 shows time series between 1972 and 1982 for the water content, Cl, pH and Cd in the aqueous phase at two depths. The results illustrate the relation between water flow and geochemical conditions in the soil. The alternation between precipitation (wet conditions) and evaporation (dry conditions) as dictated by the atmospheric conditions clearly affected the dynamics of the water content, with upward water flow during dry periods. The flow dynamics in turn significantly influenced the geochemistry near the soil surface. As illustrated, the most mobile elements (anions such as Cl^- and monovalent cations such as Na^+) move upwards during the evaporation periods, thus causing these elements to accumulate near the soil surface. The decrease in the water content near the soil surface due to evaporation produced higher concentrations and a lower pH.

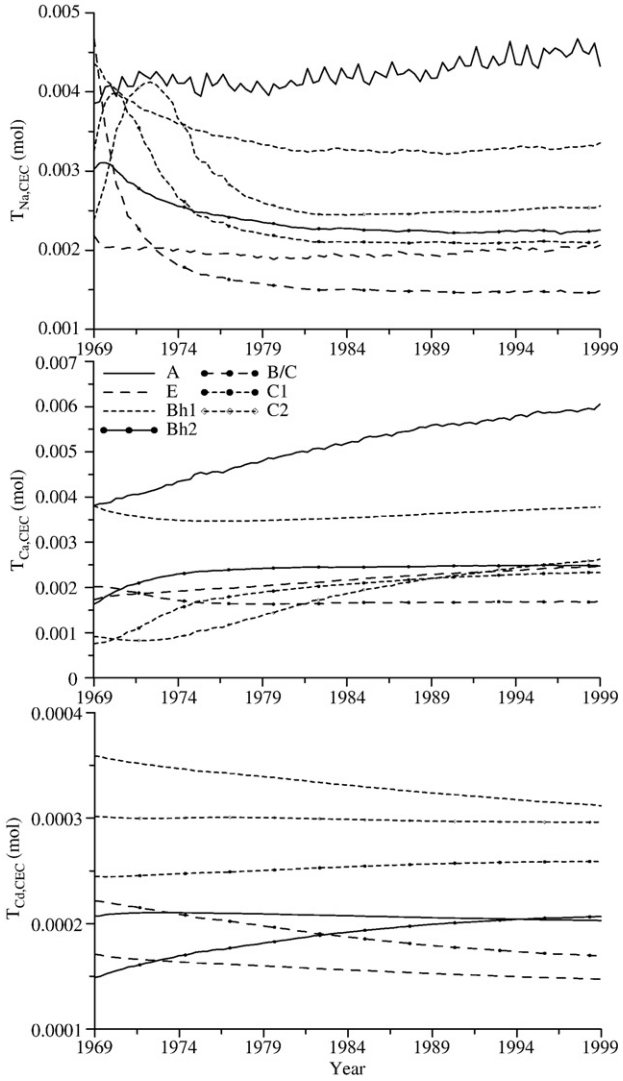

Fig. 7. $T_{Na,cec}$, $T_{Ca,cec}$ and $T_{Cd,cec}$ (mol/1000 cm^3 soil) in each horizon during the 30-year simulation (the C horizon is divided in two parts: C1 — 75 cm, and C2 — 75–100 cm).

PHREEQC calculations showed that removing only water from aqueous solutions results in a pH decrease (for a similar geochemical system, i.e., only cation exchange and equilibrium with gibbsite). Another factor intensifying the pH decrease was the greater mobility of anions (Cl^- and Br^-) compared to cations. Thus, the physical factors of decreasing water content and upward water and solute fluxes caused the pH to decrease when P_p* is negative. It should be noted that the pH in reality is also affected by other geochemical or biological processes not included in our conceptual model. For example, soil carbon dioxide concentrations that usually change in response to biological activity and moisture status of the soil can also affect soil pH (Šimůnek and Suarez, 1993).

Although upward flow during the summer had almost no effect on the total amount of heavy metals in the surface horizon due to the low mobility of these elements, the aqueous concentrations of the metals did vary significantly during the season. Several factors contribute to this. First, because of lower water contents, the concentration of all aqueous species increased during the summer period. Changes in aqueous concentrations in turn caused changes in the cation exchange equilibrium, thereby promoting monovalent cations to sorb on the cation exchange complex and bivalent cations to desorb into solution. This explains also the difference between $T_{Na,aq}$ and $T_{Ca,aq}$ during the summer near the soil surface. The aqueous concentration of Na was more controlled by the cation exchange complex than that of Ca due to preferred adsorption of Na during dry soil conditions. This (geochemical) process is further amplified by the increased supply of monovalent cations due to upward water flow during summer, leading to relatively increased sorption of the monovalent cations and higher concentrations of divalent cations and heavy metals in the soil solution. The complexation of Cd with Cl contributed also to the increase in $T_{Cd,aq}$. At a depth of 3 cm, about 0.65 and up to 3.5% of the aqueous Cd was in the form of $CdCl^+$ during winter and summer, respectively. Other Cd complexes of the form $CdCl_n^{(2-n)}$ were present in much smaller concentrations. Similar to the pH changes, changing water contents and upward fluxes both affected the amount of Cd in the aqueous phase.

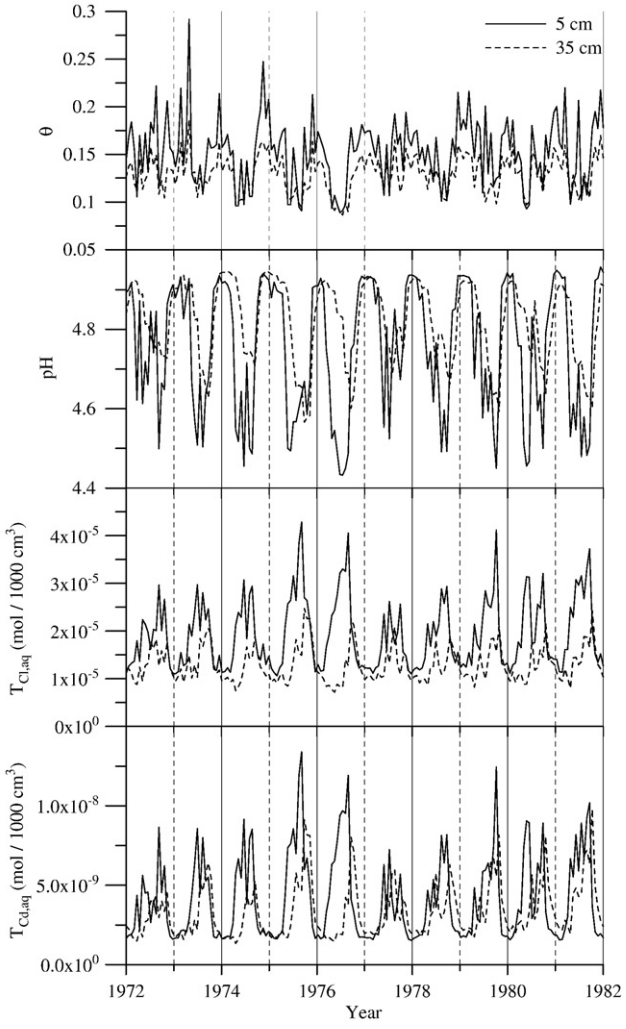

Fig. 8. Time series of water content, $T_{cl,aq}$, pH and $T_{Cd,aq}$ (mol/1000 cm^3 soil) between 1972 and 1982 at 5 cm (A-horizon) and 35 cm (Bh1-horizon).

Our results above indicate that atmospheric boundary conditions can have a significant effect on the amount and transport of Cd in a soil profile, and on its bioavailability since uptake processes by plants and soil micro-organisms are often concentration-dependent. Passive root uptake of solutes together with water uptake increases with increasing solute concentrations. Similarly, active uptake as described with Monod or Michealis–Menten kinetics will increase with increasing solute concentrations. Moreover, the high heavy metal concentrations occurred during the summer months with the highest (micro) biological activity. In addition, Cd speciation may also play a role in uptake. For example, Smolders and McLaughlin (1996) observed more Cd uptake by chard when Cl concentrations increased while the Cd^{2+} activity was kept constant, likely due to phytoavailability of $CdCl^{+}$ and other $CdCl_n^{2-n}$-species.

4. Concluding remarks

The example in this paper on heavy metal mobility shows that temporal climatic variations in precipitation and evaporation can lead to significant changes in the soil geochemical conditions, especially near the soil surface. The temporal variability in soil physical variables (water contents and fluxes as a result of changing atmospheric conditions) causes temporal variability in the geochemical variables and processes (e.g., pH, concentrations, exchange equilibria). In our example the pH decreased at lower water contents. Due to increasing concentrations at lower water contents, monovalent cations are preferred on the cation exchange complex relative to bivalent cations. Upward water fluxes during the summer, moreover, causes transport of chloride to the soil surface, which in turn leads to higher Cd concentrations in the aqueous phase due to Cd–Cl complex formation.

The example illustrates that simulators as HP1 are potentially attractive tools for studying reactive transport processes in the vadose zone during transient variably-saturated flow. Geochemical conditions are an important factor since they determine the speciation (both in the soil solution and on the solid phase) of the elements involved, and thus their mobility and bioavailability. Small variations in prevailing geochemical conditions may alter significantly the speciation and mobility of heavy metals or other constituents. Soil systems, moreover, are subject to large transient variations since they are open to the atmosphere. Hence, changes in the composition of rain water or atmospheric deposition, among other external factors, can materially alter the geochemical conditions in a soil profile.

Reactive transport codes for soil systems can therefore be helpful for unravelling processes related to pedogenesis and to model and describe pedogenesis. Although the numerical example discussed in this paper is not directly related to modelling pedogenesis, the simulations do illustrate the interactions that may occur between transient water flow and a variety of geochemical reactions, including mass transfer processes between the liquid and solid phases. The geochemical reactions together with variably-saturated water flow and drying and wetting cycles may explain many specific processes occurring during pedogenesis when extrapolated or evaluated over longer time periods. It was beside the scope of the present paper to analyze the effect of short-term fluctuations on the long-term behaviour of contaminants in the soil system. The studies of Jacques et al. (2006b, in press) revealed that there is a difference in U-leaching from soils between simulations using daily atmospheric values or long-term averaged ones. The breakthrough of U at 1 m depth occurred earlier in case of daily values.

The use of integrated reactive transport codes come with still other challenges related to (i) computational demand, (ii) updating physical properties, (iii) detail of process knowledge and model input, and (iv) model validation.

Because of relatively high computational demand, coupled codes appear mainly useful for short-time (10–1000 years) simulations. Still, the model seems suitable for evaluating soil genetic processes and genesis resulting from human impacts, such as the effect of acid rain on forest soils or the development of technosoils.

A further limitation of most current codes is that soil horizons and their properties (e.g., porosity, permeability and cation exchange properties) are considered to be static during the simulations, which is the contrary to what is needed in modelling pedogenesis. Further research should therefore address time dependency in flow and transport properties in the coupled codes.

Also, these codes combine relatively specialized information from the field of soil physics and geochemistry. Their users thus need a relatively thorough understanding of the basic physical and biogeochemical processes involved. The integrated models are also very parameter demanding, with many parameters being subject to uncertainty, including especially those in various chemical rate equations. For example, it is not straightforward under saturated conditions to relate the reactive surface area of a mineral to, for example, BET-measured surface areas (Brantley, 2003). In addition, only a small fraction of the reactive surface area will be chemically active (i.e., in contact with water) during unsaturated conditions (Kuechler and Noack, 2007). One way to address these uncertainties is by performing uncertainty and sensitivity analysis to first identify those parameters which most impact system response, thereby prioritizing parameter estimation efforts.

For the time being, only a limited number of test cases and experimental data exist for the unsaturated zone to test the full capabilities of a reactive transport code (see also Davis et al., 2004). One elaborate recent application is a study by Gonçalves et al. (2006) who successfully applied the chemistry-specific major ion geochemistry module in HYDRUS-1D (version 3.0, Šimůnek et al., 2005) to a 4-year experimental data set involving water flow and solute transport in lysimeters irrigated with waters of different quality and subjected to atmospheric conditions. Additional studies of this type should provide more credibility to the use of coupled models for addressing flow and reactive transport problems in the vadose zone.

Acknowledgements

This work was partly supported by the National Science Foundation, agreement no. EAR-9876800 and the Terrestrial Sciences Program of the Army Research Office (Terrestrial Processes and Landscape Dynamics and Terrestrial System

Modeling and Model Integration). Additional support was obtained through the bilateral agreement project "Development and evaluation of a coupled geochemical transport model between SCK•CEN and USDA-ARS (agreement no. 58-5310-0-F105), between SCK•CEN and the University of California, Riverside (agreement no. C0-90001412.01), and by the SCK•CEN R&D program on "Environmental Remediation" (project E022031 and CO91002).

References

Appelo, C.A.J., Postma, D., 2005. Geochemistry, Groundwater and Pollution, Second edition. A.A. Balkema, Rotterdam, the Netherlands.

Arkley, R.J., 1963. Calculation of carbonate and water movement in soil from climatic data. Soil Sci. 96, 239–248.

Brantley, S., 2003. Reaction kinetics of primary rock-forming minerals under ambient conditions. In: J.I. Drever (Editor), Fresh Water Geochemistry, Weathering and Soils, K.K. Turekian and H.D. Holland (Editors), Vol. 5 of Treatise on Geochemistry. Pergamon Press, Oxford, UK, pp. 73–118.

Carrayrou, J., Mosé, R., Behra, P., 2004. Operator-splitting procedures for reactive transport and comparison of mass balance errors. J. Contam. Hydrol. 68, 239–268.

Davis, J.A., Yabusaki, S.B., Steefel, C.I., Zachara, J.M., Curtis, G.P., Redden, G.B., Criscenti, L.J., and Honeyman, B.D., 2004. Assessing conceptual models for subsurface reactive transport of inorganic contaminants. EOS, 85: 449 and 455.

DeNovio, N.M., Saiers, J.E., Ryan, J.N., 2004. Colloid movement in unsaturated porous media: recent advances and future directions. Vadose Zone J. 3, 338–351.

Finke, P., 2006. Modelling the genesis of Luvisols in late Weichsel loess. In: Samouëlian, A., Cornu, S. (Eds.), Proceedings of the Workshop on Modelling of Pedogenesis, pp. 29–30.

Freedman, V.L., Bacon, D.H., Saripalli, K.P., Meyer, P.D., 2004. A film depositional model of permeability for mineral reactions in unsaturated media. Vadose Zone J. 3, 1414–1424.

Gaines, G.L., Thomas, H.C., 1953. Adsorption studies on clay minerals. II. A formulation of the thermodynamics of exchange adsorption. J. Chem. Phys. 21, 714–718.

Gonçalves, M.C., Šimůnek, J., Ramos, T.B., Martins, J.C., Neves, M.J., Pires, F.P., 2006. Multicomponent solute transport in soil lysimeters irrigated with waters of different quality. Water Resour. Res. 42, W08401. doi:10.1029/2005WR004802.

Hoosbeek, M.R., Bryant, R.B., 1992. Towards the quantitative modeling of pedogenesis — a review. Geoderma 55, 183–210.

Jacques, D., Šimůnek, J., (in preparation). User manual of the multicomponent variably-saturated transport model HP1 (Version 2.0): description, verification and examples. SCK•CEN, Mol, Belgium.

Jacques, D., Šimůnek, J., Mallants, D., van Genuchten, M.Th., 2006a. Operator-splitting errors in coupled reactive transport codes for transient variably saturated flow and contaminant transport in layered soil profiles. J. Contam. Hydrol. 88, 197–218.

Jacques, D., Šimůnek, J., Mallants, D., van Genuchten, M.Th., 2006b. Modelling uranium leaching from agricultural soils to groundwater as a criterion for comparison with complementary safety indicators. In: Van Iseghem, P. (Ed.), Scientific Basis for Nuclear Waste Management XXIX. Mat. Res. Soc. Symp. Proc., vol. 932, pp. 1057–1064.

Jacques, D., Šimůnek, J., Mallants, D., van Genuchten, M.Th., (in press). Modeling coupled hydrological and chemical processes in the vadose zone: a case study of long-term uranium transport following mineral P-fertilization. Vadose Zone J.

Jansen, B., Nierop, K.G.J., Verstraten, J.M., 2002. Influence of pH and metal/carbon ratios on soluble organic complexation of Fe(II), Fe(III) and Al in soil solutions determined by diffusive gradients in thin films. Anal. Chim. Acta 454, 259–270.

Jenny, H., 1941. Factors of Soil Formation. McGrawhill, New York, NY, USA.

Kuechler, R., Noack, K., 2007. Comparison of the solution behaviour of a pyrite-calcite mixture in batch and unsaturated sand column. J. Contam. Hydrol. 90, 203–220.

Langmuir, D., 1997. Aqueous Environmental Geochemistry. Prentice Hall, New Jersey, USA.

Lapen, D.R., Wang, C., 1999. Placic and Ortstein horizon genesis and peatland development, Southeastern Newfoundland. Soil Sci. Soc. Am. J. 63, 1472–1482.

Le Gallo, Y., Bildstein, O., Brosse, E., 1998. Coupled reaction-flow modelling of diagenetic changes in reservoir permeability, porosity and mineral compositions. J. Hydrol. 209, 366–388.

Lichtner, P.C., 1996. Continuum formulation of multicomponent-multiphase reactive transport. In: Lichtner, P.C., Steefel, C.I., Oelkers, E.H. (Eds.), Reactive Transport in Porous Media, Reviews in Mineralogy, no. 34. Mineralogical Society of America, Washington, DC, USA, pp. 1–81.

Lichtner, P.C., Yabusaki, S., Pruess, K., Steefel, C.I., 2004. Role of competitive cation exchange on chromatographic displacement of cesium in the vadose zone beneath the Hanford S/SX tank farm. Vadose Zone J. 3, 203–219.

Lin, H., 2003. Hydropedology: bridging disciplines, scales and data. Vadose Zone J. 2, 1–11.

Lin, H., Bouma, J., Pachepsky, Y., Western, A., Thompson, J., van Genuchten, M.Th., Vogel, H.-J., Lilly, A., 2006. Hydropedology: synergistic integration of pedology and hydrology. Water Resour. Res. 42, W05301. doi:10.1029/2005WR004085.

Mayer, U., 1999. A numerical model for multicomponent reactive transport in variably saturated porous media. Ph.D. thesis, Department of Earth Sciences, University of Waterloo, Waterloo, Canada.

Mayer, K.U., Frind, E.O., Blowes, D.W., 2002. Multicomponent reactive transport modelling in variably saturated porous media using a generalized formulation for kinetically controlled reactions. Water Resour. Res. 38, 1174. doi:10.1029/2001WR000682.

Mecke, M., Westman, C.J., Ilvesniemi, H., 2000. Prediction of near-saturated hydraulic conductivity in three Podzolic Boreal forest soils. Soil Sci. Soc. Am. J. 64, 485–492.

Metz, V., Pfingsten, W., Lützenkirchen, J., Schüssler, W., 2002. TrePro 2002: modelling of coupled transport reaction processes. Workshop of the Forschungszentrum Karlsruhe, 20–21 March 2002, Karlsruhe, Germany 126 p. http://www.fzk.de/fzk/groups/ine/documents/internetdokument/id_040291.pdf2002.

Millington, R.J., Quirk, J.M., 1961. Permeability of porous solids. Trans. Faraday Soc. 57, 1200–1207002E.

Morel, F., Hering, J., 1993. Principles and Applications of Aquatic Chemistry. John Wiley & Sons Inc., New York, USA.

NRC, 2006. Proceedings of the international conference on conceptual model development for subsurface reactive transport modelling of inorganic contaminants, radionuclides and nutrients, NUREG/CP-0193, Office of Nuclear Regulatory Research, U.S. Nuclear Regulatory Commission, Washington, DC, USA. http://www.iscmem.org/Documents/Proceedings_03.pdf2006.

Panda, M.N., Lake, L.W., 1995. A physical model of cementation and its effects on single-phase permeability. AAPG Bull. 79, 431–443.

Parkhurst, D.L., Appelo, C.A.J., 1999. User's guide to PHREEQC (Version 2) — a computer program for speciation, batch-reaction, one-dimensional transport, and inverse geochemical calculations. Water-Resources Investigations, Report 99-4259, Denver, Co, USA.

Penmann, H.L., 1948. Natural evaporation from open water, bare soils and grass. Proc. Royal Soc. A. 190, 120–145.

Presley, D.R., Ransom, M.D., Kluitenberg, G.J., Finnell, P.R., 2004. Effects of thirty years of irrigation on the genesis and morphology of two semi-arid soils in Kansas. Soil Sci. Soc. Am. J. 68, 1916–1926.

Rasmussen, C., Southard, R.J., Horvath, W.R., 2005. Modeling energy inputs to predict pedogenic environments using regional environmental databases. Soil Sci. Soc. Am. J. 69, 1266–1274.

Selim, H.M., Büchter, B., Hinz, C., Ma, L., 1992. Modeling the transport and retention of cadmium in soils: multireaction and multicomponent approaches. Soil Sci. Soc. Am. J. 56, 1004–1015.

Seuntjens, P., 2000. Reactive Solute Transport in Heterogeneous Porous Medium: Cadmium Leaching in Acid Sandy Soils. Ph.D., University of Antwerp, Belgium.

Seuntjens, P., Mallants, D., Toride, N., Cornelis, C., Geuzens, P., 2001. Grid lysimeter study of steady state chloride transport in two Spodosol types using TDR and wick samplers. J. Contam. Hydrol. 51, 13–39.

Šimůnek, J., Suarez, D.L., 1993. Modeling of carbon dioxide transport and production in soil: 1. Model development. Water Resour. Res. 29, 487–497.

Šimůnek, J., Jarvis, N.J., van Genuchten, M.Th., Gärdenäs, A., 2003. Review and comparison of models for describing non-equilibrium and preferential flow and transport in the vadose zone. J. Hydrol. 272, 14–35.

Šimůnek, J., van Genuchten, M.Th., Šejna, M., 2005. The HYDRUS-1D Software Package for Simulating the One-Dimensional Movement of Water, Heat, and Multiple Solutes in Variably-Saturated Media. Version 3.0, HYDRUS Software Series 1. Department of Environmental Sciences, University of California Riverside, Riverside, California, USA.

Šimůnek, J., He, C., Pang, L., Bradford, S.A., 2006a. Colloid-facilitated solute transport in variably saturated porous media: numerical model and experimental verification. Vadose Zone J. 5, 1035–1047.

Šimůnek, J., Jacques, D., van Genuchten, M.Th., Mallants, D., 2006b. Multicomponent geochemical transport modelling using HYDRUS-1D and HP1. J. Am. Water Resour. Assoc. 46, 1537–1547.

Smolders, E., McLaughlin, M.J., 1996. Chloride increases cadmium uptake in Swiss chard in a resin-buffered nutrient solution. Soil Sci. Soc. Am. J. 60, 1443–1447.

Smolders, E., Brans, K., Földi, A., Merckx, R., 1999. Cadmium fixation in soils measured by isotopic dilution. Soil Sci. Soc. Am. J. 63, 78–85.

Steefel, C.I., 2000. New directions in hydrogeochemical transport modelling: incorporating multiple kinetic and equilibrium reaction pathways. In: Bentley, L.R., Sykes, J.F., Brebbia, C.A., Gray, W.G., Pinder, G.F. (Eds.), Computational Methods in Water Resources XIII. A.A. Balkema, Rotterdam, the Netherlands, pp. 331–338.

Stolk, A.P., 2001. Landelijk Meetnet Regenwatersamenstelling, Meetresultaten 1999. RIVM, The Netherlands. RIVM Rapport 723101 056.

van Genuchten, M.Th., 1980. A closed-form equation for predicting the hydraulic conductivity of unsaturated soils. Soil Sci. Soc. Am. J. 44, 892–898.

Voegelin, A., 2001. Competitive sorption and transport of heavy metal cations in soils. Diss. ETH. No. 14101, Zürich, Switzerland.

Voegelin, A., Vulava, V., Kretzschmar, R., 2001. Reaction-based model describing competitive sorption and transport of Cd, Zn, and Ni in an acidic soil. Environ. Sci. Technol. 35, 1651–1657.

Vogel, T., Cislerova, M., Hopmans, J.W., 1991. Porous media with linearly variable hydraulic properties. Water Resour. Res. 27, 2735–2741.

Yeh, G.-T., Cheng, H.-P., 1999. 3DHYDROGEOCHEM: A 3-dimensional model of density-dependent subsurface flow and thermal multispecies-multicomponent HYDROGEOCHEMical transport. EPA/600/R-98/159.